Organometallics **1992,** *11,* 2016–2024

Transformations of 3,3-Dimethylthietane in Triosmium Cluster Complexes

Richard D. Adams,* Judy A. Belinski, and Michael P. Pompeo

Department of Chemistry and Biochemistry, University of South Carolina, Columbia, South Carolina 29208

Received November 20, 1991

Three products were isolated from the thermolysis of either $Os_3(CO)_{11}[\overline{SCH_2CMe_2CH_2}]$ (**1**) or $Os_3(CO)_{10}[\mu\text{-}\overline{SCH_2CMe_2CH_2}]$ (**2**) at 97 °C. These were identified on the basis of IR and ^1H NMR spectroscopy and single-crystal X-ray diffraction analyses as $Os_2(CO)_6[\mu\text{-}SCH_2C(Me)CH_2(CH_2)](\mu\text{-}H)$ (**3**; 14%, 18%), $Os_3(CO)_9[\mu\text{-}SCH_2C(Me)_2CH](\mu\text{-}H)$ (**4**; 18%, 21%) and $Os_4(CO)_{12}(\mu\text{-}CO)[\mu\text{-}\overline{SCH_2CMe_2CH_2}]$ (**5**; 8%, 12%). Treatment of **4** with H_2/CO (1200 psi, 5/1) at 97 °C yielded **3** (47%) and $Os_3(CO)_{10}[\mu\text{-}SCH_2CMe_3](\mu\text{-}H)$ (23%). When subjected to UV irradiation, **1** and **2** were converted to the metallacyclic isomer $Os_3(CO)_{10}[\mu\text{-}SCH_2CMe_2CH_2]$ (**6**) in 30% and 47% yields, respectively. Thermolysis of **6** at 97 °C produced **3** and **4**. Compound **6** was carbonylated (500 psi) at 70 °C to yield $Os_3(CO)_{11}[\mu\text{-}SCH_2C(Me)_2CH_2]$ (**7**; 11%) and $Os_3(CO)_{11}[\mu\text{-}SCH_2C(Me)_2CH_2C{=}O]$ (**8**; 42%), which is formed by a CO insertion into the metal–carbon bond of the metallacycle. Compound **6** reacts with $[(Et)_4N]^+Cl^-$ at 25 °C to form $[Os_3(CO)_9(\mu\text{-}SCH_2C(Me)_2CH_2)(\mu\text{-}Cl)]^-[(Et)_4N]^+$ (**9**; 87%) by decarbonylation and addition of Cl^- to the cluster. Complexes **7**–**9** were also characterized by single-crystal X-ray diffraction analyses. All three compounds contain open clusters of the three metal atoms in which the sulfur atom bridges the pair of metal atoms that are not mutually bonded. Compound **8** contains a thiametallacyclohexanone ring formed by the insertion of a CO group into the metal–carbon bond of the metallacycle in **7**. Compound **9** was formed by the cluster-opening addition of chloride to **6** and contains a bridging chloro ligand. Data for **3**: space group = $P2_1/m$, $a = 6.3804$ (8) Å, $b = 14.149$ (2) Å, $c = 8.649$ (1) Å, $\beta = 96.70$ (1)°, $Z = 2$, 1019 reflections, $R = 0.036$. Data for **4**: space group = $P\bar{1}$, $a = 9.330$ (2) Å, $b = 14.352$ (2) Å, $c = 8.656$ (2) Å, $\alpha = 93.73$ (2)°, $\beta = 117.58$ (1)°, $\gamma = 101.09$ (2)°, $Z = 2$, 1977 reflections, $R = 0.023$. Data for **7**: space group = Pn, $a = 9.791$ (2) Å, $b = 10.5812$ (9) Å, $c = 10.957$ (1) Å, $\beta = 102.09$ (1)°, $Z = 2$, 1693 reflections, $R = 0.038$. Data for **8**: space group = $P\bar{1}$, $a = 14.108$ (4) Å, $b = 16.628$ (7) Å, $c = 9.985$ (4) Å, $\alpha = 90.09$ (4)°, $\beta = 93.24$ (3)°, $\gamma = 81.97$ (3)°, $Z = 4$, 3838 reflections, $R = 0.048$. Data for **9**: space group = $P2_1/n$, $a = 9.320$ (2) Å, $b = 18.484$ (5) Å, $c = 17.943$ (3) Å, $\beta = 95.04$ (2)°, $Z = 4$, 2886 reflections, $R = 0.024$.

Introduction

Until recently, there have been very few reports describing ring-opening transformations of thietanes in discrete transition metal complexes.[1-7] Studies of the reactions of thietane A on single-crystal molybdenum surfaces under high vacuum have shown that ring opening is a very facile process.[8]

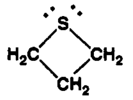

A

The reaction of *trans*-2,4-diphenylthietane with the cluster complex $Os_3(CO)_{10}(NCMe)_2$ yields cis and trans isomers of the metallacyclic complex $Os_3(CO)_{10}[\mu\text{-}SC(H)PhCH_2C(H)Ph]$ (B).[2] These complexes undergo a β-elimination reaction when heated to 97 °C, yielding the diphenylpropenethiolato complex C (eq 1).

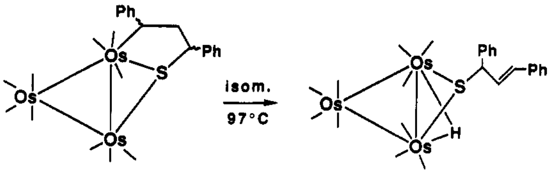

(1)

cis and *trans*-B

C

The complex $Os_3(CO)_{11}[S(CH_2)_3]$ undergoes a photoassisted ring opening accompanied by cluster decarbonylation to yield the propenethiolato complex $Os_3(CO)_{10}[\mu\text{-}SCH_2CH{=}CH_2](\mu\text{-}H)$.[1] This transformation has also been shown to proceed via a thiametallacyclic intermediate such as B.[1b] In order to study the ring-opening transformations of thietanes in the absence of β-CH activation, we have investigated the reactions of the derivative 3,3-dimethylthietane (3,3-DMT) with $Os_3(CO)_{11}(NCMe)$ and $Os_3(CO)_{10}(NCMe)_2$.[3-5] We have shown that bridging coordination of the sulfur atom promotes the nucleophile-assisted ring-opening reaction of the 3,3-DMT ligand.[4,5] Herein, we report the results of the thermally- and photolytically-induced transformations of the 3,3-DMT ligand in the complexes $Os_3(CO)_{11}[\overline{SCH_2CMe_2CH_2}]$ (**1**) and $Os_3(CO)_{10}[\mu\text{-}\overline{SCH_2CMe_2CH_2}]$ (**2**). Preliminary results of this work have been reported.[3,4a]

Experimental Section

General Data. Reagent grade solvents were stored over 4-Å molecular sieves. The compounds $Os_3(CO)_{11}NCMe$,[9] $Os_3(CO)_{10}(NCMe)_2$,[10] and 3,3-dimethylthietane[11] were prepared by the published procedures. Procedures for the preparation of $Os_3(CO)_{11}[\overline{SCH_2CMe_2CH_2}]$ (**1**) and $Os_3(CO)_{10}[\mu\text{-}\overline{SCH_2CMe_2CH_2}]$ (**2**) have been reported previously.[5] All reactions were performed under a nitrogen atmosphere unless specified otherwise. UV irradiation experiments were performed using a 360-W external high-pressure mercury lamp on reaction solutions in Pyrex glassware. Infrared spectra were recorded on a Nicolet 5DXB

---

[1] (a) Adams, R. D.; Pompeo, M. P. *Organometallics* **1990**, *9*, 1718. (b) Adams, R. D.; Pompeo, M. P. *Organometallics*, in press.

[2] Adams, R. D.; Pompeo, M. P. *Organometallics* **1992**, *11*, 103.

[3] Adams, R. D.; Pompeo, M. P. *Organometallics* **1990**, *9*, 2651.

[4] (a) Adams, R. D.; Belinski, J. A.; Pompeo, M. P. *Organometallics* **1991**, *10*, 2539. (b) Adams, R. D.; Pompeo, M. P. *Organometallics* **1992**, *11*, 1460.

[5] Adams, R. D.; Pompeo, M. P. *J. Am. Chem. Soc.* **1991**, *113*, 1619.

[6] Adams, R. D.; Belinski, J. A.; Schierlmann, J. A. *J. Am. Chem. Soc.* **1991**, *113*, 9004.

[7] Yamamoto, J. H.; Yap, G. P. A.; Jensen, C. M. *J. Am. Chem. Soc.* **1991**, *113*, 5060.

[8] Friend, C. M.; Roberts, J. T. *J. Am. Chem. Soc.* **1987**, *109*, 3872.

[9] Johnson, B. F. G.; Lewis, J.; Pippard, D. *J. Organomet. Chem.* **1978**, *160*, 263; **1981**, *213*, 249.

[10] Aime, S.; Deeming, A. J. *J. Chem. Soc., Dalton Trans.* **1983**, 1809.

[11] Searles, S.; Hays, H. R.; Lutz, E. F. *J. Org. Chem.* **1962**, *5*, 2832.

0276-7333/92/2311-2016$03.00/0

FTIR spectrophotometer. ^{1}H NMR spectra were run on either a Bruker AM-300 or AM-500 spectrometer operating at 300 or 500 MHz, respectively. Chromatographic separations were performed in air on Analtech 250-μm F_{254} silica gel HLF Uniplates. Silica gel (70–230 mesh, 60 Å) was purchased from Aldrich. Mass spectra were obtained on a VG Model 70SQ spectrometer using electron-impact ionization. Elemental analyses were performed by Desert Analytics, Tucson, AZ, or Oneida Research Services, Whitesboro, NY.

Thermolysis of 2. A solution of **2** (40 mg, 0.042 mmol) in 40 mL of heptane was heated to 97 °C for 1 h. The solvent was removed in vacuo, and the following products were separated by TLC using a 9/1 (v/v) hexane/CH_2Cl_2 solvent mixture in order of elution: colorless $Os_2(CO)_6[\mu\text{-}SCH_2C(Me)CH_2(CH_2)](\mu\text{-}H)$ (**3**; 5.0 mg, 18%), orange $Os_3(CO)_9[\mu\text{-}SCH_2CMe_2CH](\mu\text{-}H)$ (**4**; 8.0 mg, 21%), and red $Os_4(CO)_{12}(\mu\text{-}CO)[\mu\text{-}\overline{SCH_2CMe_2C}H_2]$ (**5**; 6.0 mg, 12%). A small amount of $Os_3(CO)_{12}$ was isolated from the reaction mixture. Analytical and spectral data for **3** are as follows. IR [ν(CO) (cm^{-1}) in hexane]: 2100 s, 2081 vs, 2019 s, 2014 s, 2002 s, 1977 w. ^{1}H NMR (δ in $CDCl_3$): 1.86 (s, 2 H), 1.48 (s, 3 H), 1.01 (dd, 2 H, J_{H-H} = 12 Hz, 1 Hz), 0.85 (dd, 2 H, J_{H-H} = 12 Hz, 1.5 Hz), −17.46 (t, 1 H, J_{H-H} = 1.4 Hz). ^{13}C NMR (δ in $CDCl_3$): 175.24 (2 *C*O), 170.12 (2 *C*O), 169.80 (2 *C*O), 52.05 (1 *C*H_2), 46.36 (1 *C*$(CH_2)_2CH_3$), 24.43 (1 *C*H_3), 20.55 (2 *C*H_2). Mass spectral analysis (70 eV, 60 °C): $m/z = 652 - 28x$, x = 0–6 {$[M]^+ - x(CO)$}. Anal. Calcd (found) for **3**: C, 20.30 (20.36); H, 1.55 (1.49). Analytical and spectral data for **4** are as follows. IR [ν(CO) (cm^{-1}) in hexane]: 2099 m, 2070 vs, 2050 s, 2017 sh, 2013 s, 2003 s, 1986 m, 1975 w. ^{1}H NMR (δ in $CDCl_3$): 8.55 (s, 1 H), 3.02 (dd, 1 H, J_{H-H} = 11.3 Hz, 1.7 Hz), 2.11 (d, 1 H, J_{H-H} = 11.3 Hz), 1.50 (s, 3 H), 1.31 (s, 3 H), −17.47 (d, 1 H, J_{H-H} = 1.7 Hz). Mass spectral analysis (70 eV, 120 °C): $m/z = 925 - 28x$, x = 0–9 {$[M]^+ - x(CO)$}. Analytical and spectral data for **5** are as follows. IR [ν(CO) (cm^{-1}) in hexane]: 2088 w, 2050 vs, 2040 s, 2027 m, 1997 m, 1976 w. ^{1}H NMR (δ in $CDCl_3$): 4.42 (s, 4 H), 1.64 (s, 6 H). Anal. Calcd (found) for **5**: C, 17.62 (18.22); H, 0.82 (0.82).

Thermolysis of 1. A heptane solution (40 mL) of **1** (100 mg, 0.10 mmol) was heated at 97 °C for 1 h. TLC using a 9/1 (v/v) hexane/CH_2Cl_2 solvent mixture separated the following products in order of elution: **3** (8.0 mg, 14%), **4** (7.0 mg, 18%), and **5** (8.0 mg, 8%) from unreacted **1** (12.0 mg). Yields are based on the amount of **1** consumed. A small amount of $Os_3(CO)_{12}$ precipitate was also obtained from the reaction mixture.

Photolysis of 2. A solution of **2** (40 mg, 0.042 mmol) in 40 mL of hexane was irradiated for 30 min at 25 °C. The solvent was removed in vacuo and the residue chromatographed by TLC. Elution with hexanes separated red $Os_3(CO)_{10}[\mu\text{-}SCH_2CMe_2CH_2]$ (**6**; 14 mg, 47%) from unreacted **2** (10 mg). Yields are based on the amount of **2** consumed. Analytical and spectral data for **6** are as follows. IR [ν(CO) (cm^{-1}) in hexane]: 2106 m, 2058 vs, 2045 m, 2021 vs, 2000 m, 1990 m, 1987 m, 1943, w. ^{1}H NMR (δ in $CDCl_3$): 3.08 (dd, 1 H, $^2J_{H-H}$ = 10.9 Hz, $^4J_{H-H}$ = 2.1 Hz), 2.41 (dd, 1 H, $^2J_{H-H}$ = 12.0 Hz, $^4J_{H-H}$ = 2.1 Hz), 2.10 (d, 1 H, $^2J_{H-H}$ = 12.0 Hz), 1.89 (d, 1 H, $^2J_{H-H}$ = 11.0 Hz), 1.24 (s, 3 H), 1.12 (s, 3 H). Mass spectral analysis (70 eV, 120 °C): $m/z = 954 - 28x$, x = 0–10 {$[M]^+ - x(CO)$}.

Photolysis of 1. A solution of **1** (63.5 mg, 0.064 mmol) in 50 mL of hexane was irradiated for 2 h at 25 °C. The solvent was removed in vacuo and the residue chromatographed by TLC. Elution with hexanes separated red $Os_3(CO)_{10}[\mu\text{-}SCH_2C(Me)_2CH_2]$ (**6**; 11.1 mg, 30%) from unreacted **1** (24.5 mg) and **2** (7.9 mg, 21%). Yields are based on the amount of **1** consumed.

Reaction of 4 with an H_2/CO Mixture. A solution of **4** (27 mg, 0.029 mmol) in 15 mL of heptane was placed in a 50-mL Parr autoclave. The vessel was pressurized with 1000 psi hydrogen and 200 psi carbon monoxide, sealed, and heated to 100 °C in an oil bath. After 8 h the vessel was cooled and vented. The solvent was removed in vacuo and the residue chromatographed by TLC. Elution with a 9/1 (v/v) hexane/CH_2Cl_2 solvent mixture separated the products in order of elution: **3** (7.0 mg, 47%) and yellow $Os_3(CO)_{10}[\mu\text{-}SCH_2CMe_3](\mu\text{-}H)$ (5.0 mg, 23%) from unreacted **4** (6.0 mg). Yields are based on the amount of **4** consumed. Analytical and spectral data for $Os_3(CO)_{10}[\mu\text{-}SCH_2C(Me)_3](\mu\text{-}H)$ are as follows. IR [ν(CO) (cm^{-1}) in hexane]: 2109 w, 2068 s, 2054 m, 2025 vs, 2019 m, 1999 m, 1990 m, 1983 w. ^{1}H NMR (δ in $CDCl_3$): 2.29 (s, 2 H), 1.06 (s, 9 H), −17.38 (s, 1 H). Mass spectral analysis (70 eV, 80 °C): $m/z = 956 - 28x$, x = 0–10 {$[M]^+ - x(CO)$}; m/z 956 − 71x, x = 1 {$[M]^+ - (CH_2C(Me)_3)$}.

Thermolysis of 6. A solution of **6** (19.8 mg, 0.02 mmol) in 20 mL of heptane was heated to reflux for 20 min under an nitrogen atmosphere. The solvent was removed in vacuo and the residue chromatographed by TLC. Elution with a 4/1 (v/v) hexane/CH_2Cl_2 solvent mixture separated **3** (9.0 mg, 68%) from **4** (3.5 mg, 18%).

Attempted Reaction of 4 with CO. A solution of **4** (3.7 mg, 0.004 mmol) in 5 mL of hexane was stirred at 25 °C under 1 atm of carbon monoxide. After 1 h, there was no evidence of a reaction as monitored by IR, and only **4** was obtained after TLC of the solution.

Carbonylation of 6. A solution of **6** (46.7 mg, 0.049 mmol) in 5 mL of hexane was placed in a 50-mL Parr autoclave. The vessel was pressurized to 500 psi with carbon monoxide, sealed, and heated to 70 °C in an oil bath. After 12 h, the vessel was cooled and vented. The solvent was removed in vacuo and the residue chromatographed by TLC. Elution with a 55/45 (v/v) CH_2Cl_2/hexane solvent mixture separated **3** (10.0 mg, 20%) and **4** (3.1 mg, 7%) from yellow $Os_3(CO)_{11}[\mu\text{-}SCH_2CMe_2CH_2]$ (**7**; 5.1 mg, 11%) and orange $Os_3(CO)_{11}[\mu\text{-}SCH_2CMe_2CH_2C{=}O]$ (**8**; 20.5 mg, 42%). Analytical and spectral data for **7** are as follows. IR [ν(CO) (cm^{-1}) in hexane]: 2127 w, 2081 s, 2050 vs, 2040 s, 2023 m, 2007 m, 1995 s, 1987 m, 1969 m. ^{1}H NMR (δ in $CDCl_3$): 2.30 (s, 2 H), 2.25 (s, 2 H), 1.13 (s, 6 H). Anal. Calcd (found) for **7**: C, 19.59 (19.58); H, 1.03 (0.96). Analytical and spectral data for **8** are as follows. IR [ν(CO) (cm^{-1}) in CH_2Cl_2]: 2132 m, 2090 s, 2050 vs, 2026 m, 2001 s, 1990 sh, 1615 w. ^{1}H NMR (δ in $CDCl_3$): 2.59 (s, 2 H), 2.47 (s, 2 H), 0.85 (s, 6 H). Anal. Calcd (found) for **8**: C, 20.24 (20.42); H, 1.00 (0.83).

Photolysis of 7. A solution of **7** (40.7 mg, 0.041 mmol) in 35 mL of CH_2Cl_2 was irradiated for 20 min at 25 °C. The solvent was removed in vacuo and the residue chromatographed by TLC. Elution with hexanes separated **6** (33.9 mg, 93%) from unreacted **7** (3.3 mg).

Photolysis of 8. A solution of **8** (12.5 mg, 0.012 mmol) in 15 mL of CH_2Cl_2 was irradiated for 30 min at 25 °C. The solvent was removed in vacuo and the residue chromatographed by TLC. Elution with hexanes yielded **6** (6.0 mg, 50%) and **7** (1.6 mg, 13%).

Thermolysis of 8. A solution of **8** (12.2 mg, 0.012 mmol) in 15 mL of benzene was heated to reflux for 3 h. The solvent was removed in vacuo, and the residue was chromatographed by TLC. Elution with a 4/1 (v/v) hexane/CH_2Cl_2 solvent mixture yielded the following in order of elution: **3** (7.0 mg, 70%) and **7** (1.9 mg, 16%).

Reaction of 6 with Tetraethylammonium Chloride. A 4.0-mg (0.022-mmol) amount of $[(Et)_4N]^+Cl^-\cdot H_2O$ dissolved in 1.0 mL of CH_3CN was added to a solution of **6** (20.0 mg, 0.021 mmol) in 20 mL of CH_2Cl_2 at 25 °C. The color of the solution changed from red to orange over a period of 9 h. The solvent was then reduced in volume, and hexane (10 mL) was added to precipitate orange $Os_3(CO)_9(\mu\text{-}Cl)[\mu\text{-}SCH_2CMe_2CH_2]^-[C_2H_5)_4N]^+$ (**9**; 18 mg, 87%). Subsequent TLC of the mother liquor yielded 2.0 mg of unreacted **6**. The yield of **9** is based on amount of **6** consumed. Analytical and spectral data for **9** are as follows. For **9** are as follows. IR [ν(CO) (cm^{-1}) in CH_2Cl_2]: 2073 m, 2029 vs, 1983 s, 1975 s, 1965 m, 1957 m, 1883 w. ^{1}H NMR (δ in CH_2Cl_2): 3.17 (q, 8 H), 2.52 (dd, 2 H, $^2J_{H-H}$ = 11 Hz, $^4J_{H-H}$ = 1 Hz), 1.65 (dd, 2 H, $^2J_{H-H}$ = 11 Hz, $^4J_{H-H}$ = 1 Hz), 1.42 (s, 3 H), 1.32 (m, 12 H), 1.26 (s, 3 H). Anal. Calcd (found) for **9**: C, 24.23 (24.20); H, 2.77 (2.62); N, 1.28 (1.26).

Crystallographic Analyses

Colorless crystals of **3** were grown by slow evaporation of a pentane solution at 25 °C. Orange crystals of **4** were grown from a concentrated hexane solution under a nitrogen atmosphere at 25 °C. Yellow crystals of **7** and orange crystals of **8** were grown by slow evaporation of hexane/CH_2Cl_2 solvent mixtures at 25 °C. Orange crystals of **9** were grown from a 1/3 hexane/CH_2Cl_2 solvent mixture at −14 °C. The data crystals were mounted in thin-walled glass capillaries. Diffraction measurements were made on a Rigaku AFC6S fully automated four-circle diffractometer using graphite-monochromatized Mo Kα radiation. Unit cells were determined and refined from 15 randomly selected reflections ob-

Table I. Crystallographic Data for Diffraction Studies

	compd				
	3	4	7	8	9
empirical formula	$Os_2SO_6C_{11}H_{10}$	$Os_3SO_9C_{14}H_{10}$	$Os_3SO_{11}C_{16}H_{10}$	$Os_3SO_{12}C_{17}H_{10}$	$Os_3ClSO_9NC_{22}H_{30}$
mol wt	650.66	924.89	908.91	1008.92	1090.59
cryst system	monoclinic	triclinic	monoclinic	triclinic	monoclinic
lattice params					
a (Å)	6.3804 (8)	9.330 (2)	9.791 (2)	14.108 (4)	9.320 (2)
b (Å)	14.149 (2)	14.352 (2)	10.5812 (9)	16.628 (7)	18.484 (5)
c (Å)	8.649 (1)	8.656 (2)	10.957 (1)	9.985 (4)	17.943 (3)
α (deg)		93.73 (2)		90.09 (4)	
β (deg)	96.70 (1)	117.58 (1)	102.09 (1)	93.24 (3)	95.04 (2)
γ (deg)		101.09 (2)		81.97 (3)	
V (Å^3)	775.5 (3)	992.3 (4)	1110.0 (3)	2316 (3)	3079 (1)
space group	$P2_1/m$ (No. 11)	$P\bar{1}$ (No. 2)	Pn (No. 7)	$P\bar{1}$ (No. 2)	$P2_1/c$ (No. 14)
Z value	2	2	2	4	4
D_{calc} (g/cm^3)	2.79	3.10	2.93	2.89	2.35
$F(000)$	584	820	876	1808	2008
μ(Mo, Kα) (cm^{-1})	165.33	193.24	172.89	165.83	125.59
temp (°C)	20	20	20	20	20
$2\theta_{max}$ (deg)	46.0	43.0	47.9	40.8	45.0
no. of observns ($I > 3\sigma(I)$)	1019	1977	1693	3838	2886
no. of variables	99	271	278	425	334
residuals: R, R_w	0.036, 0.043	0.023, 0.025	0.038, 0.043	0.048, 0.055	0.024, 0.026
goodness of fit indicator	2.88	1.42	2.78	3.20	1.27
max shift in final cycle	0.11	0.06	0.12	0.01	0.00
largest peak in final diff map (e/Å^3)	2.10	0.96	1.86	1.96	0.73
abs corr	analytical	analytical	empirical	analytical	empirical

tained by using the AFC6 automatic search, center, index, and least-squares routines. Crystal data, data collection parameters, and results of the analyses are listed in Table I. All data processing was performed on a Digital Equipment Corp. VAXstation 3520 computer by using the TEXSAN structure-solving program library obtained from the Molecular Structure Corp., The Woodlands, TX. Neutral-atom scattering factors were calculated by the standard procedures.[12a] Anomalous dispersion corrections were applied to all non-hydrogen atoms.[12b] Lorentz–polarization (Lp) and absorption corrections were applied in each analysis. Full-matrix least-squares refinements minimized the function

$$\sum_{hkl} w(|F_o| - |F_c|)^2$$

where $w = 1/\sigma(F)^2$, $\sigma(F) = \sigma(F_o^2)/2F_o$, and $\sigma(F_o^2) = [\sigma(I_{raw})^2 + (0.02I_{net})^2]^{1/2}/Lp$.

Compound 3 crystallized in the monoclinic crystal system. The systematic absences $0k0$, $k = 2n + 1$, were indicative of either of the space groups $P2_1/m$ or $P2_1$. The centrosymmetric space group $P2_1/m$ was tried initially and confirmed by the successful solution and refinement of the structure. The structure was solved by a combination of direct methods (MITHRIL) and difference Fourier syntheses. All non-hydrogen atoms were refined with anisotropic thermal parameters. Since $Z = 2$, the molecule contains a crystallographically imposed mirror plane of symmetry. The hydride ligand was located crystallographically and was refined (position only). The positions of the remaining hydrogen atoms were calculated by assuming idealized geometries. Their contributions were added to the structure factor calculations, but their positions were not refined.

Compound 4 crystallized in the triclinic crystal system. The centrosymmetric space group $P\bar{1}$ was assumed and confirmed by successful solution and refinement of the structure. The structure was solved by a combination of direct methods (MITHRIL) and difference Fourier syntheses. All non-hydrogen atoms were refined with anisotropic thermal parameters. The hydride ligand was located crystallographically. The positions of the remaining hydrogen atoms were calculated by assuming idealized geometries. Their contributions were added to the structure factor calculations, but their positions were not refined.

Compound 7 crystallized in the monoclinic crystal system. The systematic absences in the data were consistent with either of the space groups $P2/n$ or Pn. Since $Z = 2$, the noncentric space group Pn was assumed initially and confirmed by the successful solution and refinement of the structure. The structure was solved by a combination of direct methods (MITHRIL) and difference Fourier syntheses. All non-hydrogen atoms were refined with anisotropic thermal parameters. The positions of the hydrogen atoms were calculated by assuming idealized geometries. Their contributions were added to the structure factor calculations, but their positions were not refined.

Compound 8 crystallized in the triclinic crystal system with two independent molecules in the unit cell. The centrosymmetric space group $P\bar{1}$ was assumed and confirmed by successful solution and refinement of the structure. The structure was solved by a combination of direct methods (MITHRIL) and difference Fourier syntheses. All atoms heavier than carbon were refined with anisotropic thermal parameters. The positions of the hydrogen atoms were calculated by assuming idealized geometries. Their contributions were added to the structure factor calculations, but their positions were not refined.

Compound 9 crystallized in the monoclinic crystal system. The space group $P2_1/c$ was identified uniquely on the basis of the systematic absences observed during the collection of data. The structure was solved by a combination of direct methods (MITHRIL) and difference Fourier syntheses. All remaining non-hydrogen atoms were subsequently obtained from difference Fourier syntheses and were refined with anisotropic thermal parameters. The positions of all hydrogen atoms were calculated by assuming idealized geometries. Their contributions were added to the structure factor calculations, but their positions were not refined.

Results

Thermolysis of either 1 or 2 at 97 °C produced complexes 3–5 in yields of 14–18%, 18–21%, and 8–12%, respectively; see Scheme I. Each of these products was characterized by IR, ^{1}H NMR, and a single-crystal X-ray diffraction analysis. An ORTEP drawing of the molecular structure of 3 is shown in Figure 1. Final atomic positional parameters are listed in Table II. Selected interatomic distances and angles are listed in Tables III and IV. The molecule contains only two metal atoms. Three terminal carbonyl ligands are bound to each metal atom. The metal–metal bond, Os(1)–Os(1) = 2.9576 (9) Å, is bridged by the sulfur atom S(1) and a hydride ligand H (δ = −17.45 ppm). There is also a methylene group bonded to each metal atom, Os(1)–C(3) = 2.18 (1) Å, and the sulfur atom, S(1)–C(1) = 1.81 (2) Å, and all three methylene groups are connected by a CMe group. The molecule contains a

---

[12] (a) *International Tables for X-ray Crystallography*; Kynoch Press: Birmingham, England, 1975; Vo. IV, Table 2.2B, pp 99–101. (b) *Ibid.*, Table 2.3.1, pp 149–150.

Table II. Positional Parameters and *B*(eq) Values (Å^2) for $Os_2(CO)_6[S(CH_2C(CH_2)_2CH_3](H)$ (3)

atom	*x*	*y*	*z*	*B*(eq)
Os(1)	0.71618 (07)	0.35451 (03)	0.24746 (06)	3.00 (3)
S(1)	0.9604 (06)	$^1/_4$	0.1406 (05)	3.1 (2)
O(11)	0.986 (02)	0.3667 (08)	0.5681 (14)	7.4 (7)
O(12)	0.3324 (17)	0.4549 (08)	0.3463 (16)	7.3 (7)
O(13)	0.8946 (16)	0.5362 (06)	0.1301 (12)	5.4 (5)
C(1)	0.846 (03)	$^1/_4$	−0.061 (02)	3.7 (8)
C(2)	0.610 (03)	$^1/_4$	−0.067 (02)	3.4 (7)
C(3)	0.540 (02)	0.3377 (08)	0.0173 (16)	3.7 (6)
C(4)	0.501 (04)	$^1/_4$	−0.234 (03)	6 (1)
C(11)	0.885 (02)	0.3610 (09)	0.4505 (19)	4.7 (7)
C(12)	0.478 (02)	0.4170 (08)	0.3130 (17)	4.5 (7)
C(13)	0.827 (02)	0.4681 (09)	0.1745 (16)	4.1 (6)
H	0.66 (02)	$^1/_4$	0.208 (18)	3.0

Table III. Intramolecular Distances for 3^a

Os(1)–H	1.55 (4)	Os(1)–Os(1)′	2.9576 (9)
Os(1)–C(13)	1.89 (1)	S(1)–C(1)	1.81 (2)
Os(1)–C(12)	1.90 (1)	O–C(av)	1.14 (2)
Os(1)–C(11)	1.95 (2)	C(1)–C(2)	1.50 (2)
Os(1)–C(3)	2.18 (1)	C(2)–C(3)	1.53 (2)
Os(1)–S(1)	2.410 (3)	C(2)–C(4)	1.53 (3)

^{a} Distances are in angstroms. Estimated standard deviations in the least significant figure are given in parentheses.

Table IV. Intramolecular Bond Angles for 3^a

C(13)–Os(1)–C(12)	92.6 (5)	C(3)–Os(1)–S(1)	82.6 (4)
C(13)–Os(1)–C(11)	94.2 (6)	C(3)–Os(1)–Os(1)	83.8 (3)
C(13)–Os(1)–C(3)	87.8 (5)	S(1)–Os(1)–Os(1)	52.14 (6)
C(13)–Os(1)–S(1)	96.3 (4)	C(1)–S(1)–Os(1)	99.3 (5)
C(13)–Os(1)–Os(1)	148.1 (4)	Os(1)–S(1)–Os(1)	75.7 (1)
C(12)–Os(1)–C(11)	94.9 (6)	C(2)–C(1)–S(1)	109 (1)
C(12)–Os(1)–C(3)	88.7 (6)	C(1)–C(2)–C(3)	109 (1)
C(12)–Os(1)–S(1)	167.2 (4)	C(1)–C(2)–C(4)	112 (2)
C(12)–Os(1)–Os(1)	117.7 (4)	C(3)–C(2)–C(3)	108 (2)
C(11)–Os(1)–C(3)	175.8 (5)	C(3)–C(2)–C(4)	109 (1)
C(11)–Os(1)–S(1)	93.5 (4)	C(2)–C(3)–Os(1)	111.9 (9)
C(11)–Os(1)–Os(1)	92.7 (4)	O–C–Os(av)	178 (1)

^{a} Angles are in degrees. Estimated standard deviations in the least significant figure are given in parentheses.

Table V. Positional Parameters and *B*(eq) Values (Å^2) for $Os_3(CO)_9[SCH_2CMe_2CH](H)$ (4)

atom	*x*	*y*	*z*	*B*(eq)
Os(1)	0.05670 (06)	0.15116 (03)	−0.19171 (06)	2.48 (2)
Os(2)	0.03756 (06)	0.34570 (03)	−0.18040 (06)	2.80 (2)
Os(3)	0.28961 (06)	0.27820 (03)	−0.25208 (06)	2.88 (2)
S	0.0673 (04)	0.14692 (19)	−0.4671 (04)	3.3 (1)
O(11)	−0.2265 (13)	−0.0192 (07)	−0.2545 (13)	6.2 (4)
O(12)	0.3102 (12)	0.0278 (07)	−0.0564 (11)	5.4 (4)
O(13)	0.1346 (15)	0.2150 (07)	0.1869 (13)	6.9 (5)
O(21)	0.3165 (12)	0.4813 (06)	0.1640 (12)	5.4 (4)
O(22)	−0.0797 (15)	0.5074 (07)	−0.3672 (14)	7.5 (5)
O(23)	−0.1815 (13)	0.3396 (06)	−0.0070 (14)	6.2 (4)
O(31)	0.5297 (13)	0.1518 (07)	−0.1973 (17)	7.6 (5)
O(32)	0.3895 (13)	0.3855 (07)	−0.4945 (13)	6.8 (4)
O(33)	0.5625 (11)	0.4121 (06)	0.0866 (12)	4.8 (3)
C(1)	−0.1019 (17)	0.1992 (09)	−0.6081 (16)	4.1 (5)
C(2)	−0.2323 (15)	0.1907 (08)	−0.5496 (15)	3.4 (4)
C(3)	−0.1488 (14)	0.2201 (07)	−0.3480 (14)	3.1 (4)
C(4)	−0.351 (02)	0.2554 (11)	−0.636 (02)	6.0 (6)
C(5)	−0.3422 (19)	0.0877 (10)	−0.609 (02)	4.9 (6)
C(11)	−0.1257 (16)	0.0448 (08)	−0.2383 (16)	3.7 (5)
C(12)	0.2220 (15)	0.0766 (08)	−0.1066 (14)	3.3 (4)
C(13)	0.1042 (16)	0.1935 (08)	0.0443 (18)	4.1 (5)
C(21)	0.2242 (15)	0.4304 (08)	0.0333 (16)	3.3 (4)
C(22)	−0.0367 (18)	0.4461 (09)	−0.2936 (18)	4.9 (5)
C(23)	−0.0962 (15)	0.3428 (07)	−0.0711 (16)	3.6 (4)
C(31)	0.4397 (15)	0.1989 (09)	−0.2193 (18)	4.4 (5)
C(32)	0.3542 (17)	0.3454 (09)	−0.4035 (17)	4.4 (5)
C(33)	0.4545 (15)	0.3627 (08)	−0.0396 (16)	3.1 (4)
H(1)	0.114 (12)	0.344 (06)	−0.315 (12)	3.0

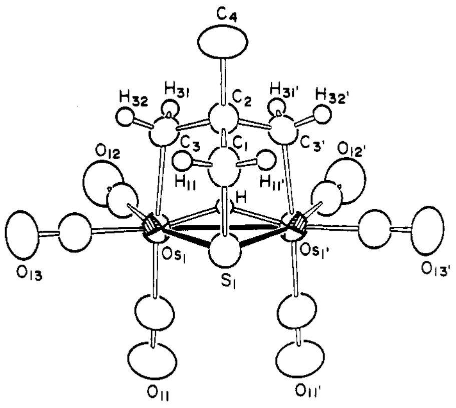

Figure 1. ORTEP diagram of $Os_2(CO)_6(\mu\text{-}H)[\mu\text{-}S(CH_2)_3CH_3]$ (3), showing 50% probability thermal ellipsoids.

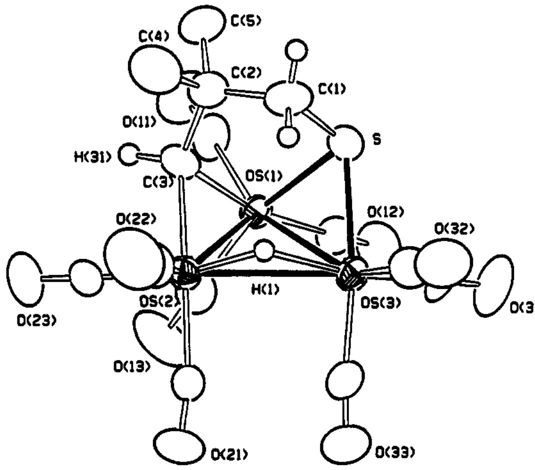

Figure 2. ORTEP diagram of $Os_3(CO)_9(\mu\text{-}H)[\mu\text{-}SCH_2CMe_2CH]$ (4), showing 50% probability thermal ellipsoids.

Table VI. Intramolecular Distances for 4^a

Os(1)–C(13)	1.91 (1)	Os(2)–Os(3)	3.0006 (8)
Os(1)–C(11)	1.92 (1)	Os(3)–H(1)	1.93 (9)
Os(1)–C(12)	1.94 (1)	Os(3)–C(33)	1.90 (1)
Os(1)–C(3)	2.23 (1)	Os(3)–C(31)	1.90 (1)
Os(1)–S	2.429 (3)	Os(3)–C(32)	1.92 (1)
Os(1)–Os(3)	2.8233 (8)	Os(3)–S	2.404 (3)
Os(1)–Os(2)	2.8301 (7)	S–C(1)	1.83 (1)
Os(2)–H(1)	1.63 (9)	O–C(av)	1.14 (2)
Os(2)–C(22)	1.86 (1)	C(1)–C(2)	1.51 (2)
Os(2)–C(23)	1.88 (1)	C(2)–C(5)	1.53 (2)
Os(2)–C(21)	1.96 (1)	C(2)–C(3)	1.53 (1)
Os(2)–C(3)	2.12 (1)	C(2)–C(4)	1.54 (2)

^{a} Distances are in angstroms. Estimated standard deviations in the least significant figure are given in parentheses.

Table VII. Selected Intramolecular Bond Angles for 4^a

C(13)–Os(1)–S	160.7 (4)	C(22)–Os(2)–Os(3)	114.8 (4)
C(11)–Os(1)–S	105.0 (4)	C(21)–Os(2)–Os(1)	112.2 (3)
C(21)–Os(2)–Os(3)	88.1 (3)	C(3)–Os(2)–Os(1)	51.2 (3)
C(12)–Os(1)–S	89.9 (3)	C(3)–Os(2)–Os(3)	90.3 (3)
C(3)–Os(1)–S	79.1 (3)	Os(1)–Os(2)–Os(3)	57.83 (2)
C(33)–Os(3)–S	164.6 (3)	C(33)–Os(3)–Os(1)	110.7 (3)
C(3)–Os(1)–Os(3)	92.8 (3)	C(33)–Os(3)–Os(2)	86.4 (3)
C(3)–Os(1)–Os(2)	47.7 (3)	C(31)–Os(3)–S	82.2 (4)
S–Os(1)–Os(3)	53.86 (7)	C(32)–Os(3)–S	100.1 (4)
S–Os(1)–Os(2)	92.04 (7)	Os(3)–Os(1)–Os(2)	64.11 (2)
C(32)–Os(3)–Os(2)	116.1 (4)	S–Os(3)–Os(1)	54.65 (7)
Os(1)–Os(3)–Os(2)	58.05 (2)	S–Os(3)–Os(2)	88.46 (7)
C(1)–S–Os(3)	106.8 (4)	C(1)–S–Os(1)	104.4 (4)
Os(3)–S–Os(1)	71.49 (8)	C(2)–C(1)–S	111.2 (8)
C(1)–C(2)–C(3)	110 (1)	Os(2)–C(3)–Os(1)	81.1 (4)
O–C–Os(av)	177 (2)		

^{a} Angles are in degrees. Estimated standard deviations in the least significant figure are given in parentheses.

Table VIII. Positional Parameters and *B*(eq) Values (Å²) for 7

atom	*x*	*y*	*z*	*B*(eq)
Os(1)	0.7288	0.37660 (8)	0.8899	2.33 (4)
Os(2)	0.7671 (2)	0.2216 (1)	0.6752 (1)	2.32 (4)
Os(3)	0.6844 (1)	0.01159 (9)	0.8237 (1)	2.36 (4)
S	0.7662 (7)	0.1694 (6)	0.9849 (6)	2.6 (2)
O(11)	1.046 (3)	0.434 (3)	1.008 (3)	7 (1)
O(12)	0.417 (2)	0.358 (2)	0.811 (3)	6 (1)
O(13)	0.728 (3)	0.643 (2)	0.787 (2)	5 (1)
O(21)	0.841 (3)	0.042 (3)	0.477 (3)	6 (1)
O(22)	0.839 (3)	0.469 (2)	0.556 (3)	6 (1)
O(23)	0.465 (2)	0.262 (3)	0.556 (2)	5 (1)
O(24)	1.084 (3)	0.224 (3)	0.822 (3)	7 (2)
O(31)	0.638 (3)	−0.189 (2)	1.008 (3)	6 (1)
O(32)	0.644 (3)	−0.159 (2)	0.591 (2)	5 (1)
O(33)	0.384 (3)	0.094 (2)	0.753 (3)	6 (1)
O(34)	1.006 (2)	−0.051 (2)	0.866 (2)	5 (1)
C(1)	0.654 (3)	0.193 (2)	1.100 (2)	3 (1)
C(2)	0.697 (3)	0.318 (3)	1.164 (3)	3 (1)
C(3)	0.689 (3)	0.428 (2)	1.070 (3)	4 (1)
C(4)	0.850 (3)	0.299 (3)	1.241 (3)	4 (1)
C(5)	0.600 (4)	0.344 (4)	1.253 (4)	6 (2)
C(11)	0.932 (3)	0.405 (3)	0.964 (3)	4 (1)
C(12)	0.539 (4)	0.358 (3)	0.835 (3)	3 (1)
C(13)	0.730 (3)	0.538 (3)	0.829 (3)	4 (1)
C(21)	0.818 (3)	0.111 (3)	0.554 (3)	4 (1)
C(22)	0.820 (3)	0.376 (3)	0.607 (3)	4 (1)
C(23)	0.580 (4)	0.245 (3)	0.601 (3)	4 (1)
C(24)	0.971 (4)	0.223 (4)	0.772 (3)	5 (2)
C(31)	0.657 (3)	−0.114 (3)	0.939 (3)	3 (1)
C(32)	0.669 (4)	−0.092 (3)	0.674 (2)	4 (1)
C(33)	0.505 (4)	0.066 (2)	0.781 (3)	3 (1)
C(34)	0.893 (3)	−0.024 (3)	0.848 (3)	4 (1)

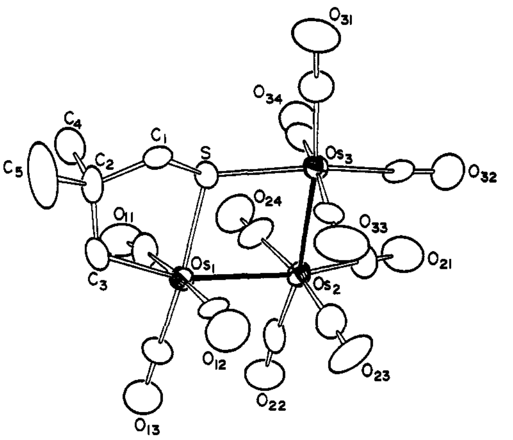

Figure 3. ORTEP diagram of $Os_3(CO)_{11}[\mu\text{-}SCH_2CMe_2CH_2]$ (7), showing 50% probability thermal ellipsoids.

Table IX. Intramolecular Distances for 7[a]

Os(1)–Os(2)	2.955 (1)	Os(2)–C(24)	2.05 (4)
Os(1)–Os(3)	3.937 (2)	Os(3)–S	2.441 (6)
Os(1)–S	2.421 (6)	Os(3)–C(31)	1.89 (3)
Os(1)–C(3)	2.16 (3)	Os(3)–C(32)	1.95 (3)
Os(1)–C(11)	2.00 (3)	Os(3)–C(33)	1.82 (3)
Os(1)–C(12)	1.84 (4)	Os(3)–C(34)	2.04 (3)
Os(1)–C(13)	1.83 (3)	S–C(1)	1.85 (3)
Os(2)–Os(3)	2.966 (2)	C(1)–C(2)	1.52 (4)
Os(2)–C(21)	1.91 (3)	C(2)–C(3)	1.55 (4)
Os(2)–C(22)	1.91 (3)	O–C(av)	1.16 (4)
Os(2)–C(23)	1.85 (4)		

[a] Distances are in angstroms. Estimated standard deviations in the least significant figure are given in parentheses.

Table X. Intramolecular Bond Angles for 7[a]

Os(2)–Os(1)–S	78.9 (2)	Os(3)–Os(2)–C(23)	89 (1)
Os(2)–Os(1)–C(3)	160.8 (8)	Os(3)–Os(2)–C(24)	94 (1)
Os(2)–Os(1)–C(11)	97 (1)	Os(2)–Os(3)–S	78.4 (2)
Os(2)–Os(1)–C(12)	88 (1)	Os(2)–Os(3)–C(31)	171 (1)
Os(2)–Os(1)–C(13)	102 (1)	Os(2)–Os(3)–C(32)	86.8 (8)
S–Os(1)–C(3)	82.8 (7)	Os(2)–Os(3)–C(33)	88.9 (8)
S–Os(1)–C(11)	85 (1)	Os(2)–Os(3)–C(34)	80.0 (8)
S–Os(1)–C(12)	95.3 (8)	S–Os(3)–C(31)	94 (1)
S–Os(1)–C(13)	171 (1)	S–Os(3)–C(32)	162 (1)
C(3)–Os(1)–C(11)	87 (1)	S–Os(3)–C(33)	97 (1)
C(3)–Os(1)–C(12)	88 (1)	S–Os(3)–C(34)	82 (1)
C(3)–Os(1)–C(13)	97 (1)	Os(1)–S–Os(3)	108.2 (2)
Os(1)–Os(2)–Os(3)	83.35 (4)	Os(1)–S–C(1)	96.7 (8)
Os(1)–Os(2)–C(21)	171 (1)	Os(3)–S–C(1)	116 (1)
Os(1)–Os(2)–C(22)	85.7 (8)	S–C(1)–C(2)	107 (2)
Os(1)–Os(2)–C(23)	90 (1)	C(1)–C(2)–C(3)	112 (2)
Os(1)–Os(2)–C(24)	82 (1)	Os(1)–C(3)–C(2)	115 (2)
Os(3)–Os(2)–C(21)	94 (1)	Os–C–O(av)	175 (3)
Os(3)–Os(2)–C(22)	169.0 (8)		

[a] Angles are in degrees. Estimated standard deviations in the least significant figure are given in parentheses.

crystallographically imposed reflection plane that passes through atoms S(1), C(1), C(2), C(4), and H.

An ORTEP drawing of the molecular structure of 4 is shown in Figure 2. Final atomic positional parameters are listed in Table V. Selected interatomic distances and angles are listed in Tables VI and VII. The molecule contains a closed triangular cluster of three metal atoms with nine terminal carbonyl ligands. A SCH_2CMe_2CH ligand bridges one face of the cluster with the sulfur atom S(1) bridging the Os(1)–Os(3) edge and the alkylidene carbon, C(3), bridging the Os(1)–Os(2) edge, Os(2)–C(3) = 2.12 (1) Å and Os(1)–C(3) = 2.23 (1) Å. The third edge is bridged by a hydride ligand (located crystallographically, $\delta = -17.46$ ppm).

Compound 5 is structurally very similar to its ruthenium homolog that has been obtained from the reaction of 3,3-DMT with $Ru_3(CO)_{12}$.[13] It contains a 3,3-DMT ligand bridging the wing-tips of a butterfly tetrahedron through the sulfur atom. Details of the structural analysis of 5 will be published in a forthcoming report.[14]

Treatment of 4 with a 5/1 mixture of H_2/CO (1200 psi) at 100 °C yielded 3 (47%) and the neopentanethiolato complex $Os_3(CO)_{10}[\mu\text{-}SCH_2CMe_3)](\mu\text{-}H)$ (23%). The latter was characterized by IR, ^1H NMR, and mass spectrometry and is believed to be structurally similar to a number of related compounds with the formula $Os_3(CO)_{10}(\mu\text{-}SR)(\mu\text{-}H)$ that were reported previously.[15]

UV irradiation of either 1 or 2 yielded the isomer $Os_3(CO)_{10}[\mu\text{-}SCH_2C(Me)_2CH_2]$ (6; 30%, 47%). We were unable to obtain crystals of 6 for a structural characterization, but on the basis of its ^1H NMR spectrum and the close similarity of its IR spectrum to the structurally characterized *cis*-2,4-diphenylthietane analog B,[2] it is believed that 6 has a structure consisting of a thiametallacyclic ring and a closed triangular cluster of three osmium atoms (see Scheme II). This is also supported by the nature of the products obtained from its reactions and thermal transformations. For example, thermolysis of 6 at 97 °C yielded complexes 3 and 4.

Complex 6 added CO at 700 psi/70 °C to yield the two products $Os_3(CO)_{11}[\mu\text{-}SCH_2C(Me)_2CH_2]$ (7) and $Os_3(CO)_{11}[\mu\text{-}SCH_2C(Me)_2CH_2C{=}O]$ (8), both of which have been characterized crystallographically. An ORTEP drawing of the molecular structure of 7 is shown in Figure 3. Final atomic positional parameters are listed in Table VIII. Selected interatomic distances and angles are listed in

---

(13) Adams, R. D.; Belinski, J. A. *J. Cluster Sci.* **1990**, *1*, 319.

(14) Data for 5: space group = $P\bar{1}$, a = 10.205 (4) Å, b = 14.399 (2) Å, c = 9.342 (2) Å, α = 92.52 (2)°, β = 108.89 (3)°, γ = 85.82 (2)°, Z = 2, 2678 reflections, and R = 0.029. Adams, R. D.; Belinski, J. A. *Organometallics*, submitted for publication.

(15) Johnson, B. F. G.; Lewis, J.; Kitty, O. A. *J. Chem. Soc. A* **1968**, 2859.

Table XI. Positional Parameters and *B*(eq) Values (Å^2) for 8

atom	*x*	*y*	*z*	*B*(eq)
Os(1)	0.23563 (08)	0.10663 (05)	0.04465 (09)	3.53 (6)
Os(2)	0.16189 (08)	0.04219 (05)	−0.21658 (09)	3.34 (5)
Os(3)	0.23684 (08)	0.18202 (05)	−0.33000 (09)	3.03 (5)
Os(4)	0.77377 (08)	0.39020 (05)	0.50938 (09)	3.49 (6)
Os(5)	0.84058 (08)	0.45649 (05)	0.25782 (09)	3.42 (5)
Os(6)	0.76657 (08)	0.31545 (05)	0.13438 (09)	3.03 (5)
S(1)	0.3226 (05)	0.1780 (03)	−0.1095 (06)	3.3 (3)
S(2)	0.6825 (05)	0.3211 (03)	0.3421 (06)	3.1 (3)
O(11)	0.4192 (16)	−0.0137 (11)	0.0981 (19)	7 (1)
O(12)	0.1387 (17)	0.0049 (12)	0.2336 (19)	8 (1)
O(13)	0.0520 (15)	0.2310 (11)	0.0477 (17)	6 (1)
O(14)	0.3238 (16)	0.1360 (11)	0.3137 (17)	7 (1)
O(21)	0.1085 (15)	−0.0416 (10)	−0.4755 (18)	6 (1)
O(22)	0.3687 (14)	−0.0477 (10)	−0.2024 (18)	5 (1)
O(23)	−0.0346 (14)	0.1544 (09)	−0.2144 (19)	6 (1)
O(24)	0.0871 (16)	−0.0794 (10)	−0.0369 (17)	6 (1)
O(31)	0.3138 (15)	0.3284 (09)	−0.4495 (16)	6 (1)
O(32)	0.1143 (14)	0.1546 (10)	−0.5850 (18)	6 (1)
O(33)	0.4089 (14)	0.0625 (10)	−0.4205 (17)	5 (1)
O(34)	0.0759 (13)	0.3013 (09)	−0.2139 (17)	5 (1)
O(41)	0.8782 (17)	0.4843 (11)	0.7139 (19)	7 (1)
O(42)	0.5957 (16)	0.5191 (12)	0.543 (02)	7 (1)
O(43)	0.9536 (14)	0.2643 (10)	0.5363 (18)	6 (1)
O(44)	0.6882 (16)	0.3604 (12)	0.7640 (18)	7 (1)
O(51)	1.0352 (14)	0.3458 (10)	0.2888 (17)	5 (1)
O(52)	0.6318 (14)	0.5433 (10)	0.2417 (19)	6 (1)
O(53)	0.8943 (16)	0.5428 (11)	0.0065 (16)	6 (1)
O(54)	0.9129 (15)	0.5798 (09)	0.4490 (17)	6 (1)
O(61)	0.6864 (14)	0.1726 (09)	−0.0011 (17)	5 (1)
O(62)	0.5931 (15)	0.4333 (09)	0.0111 (19)	6 (1)
O(63)	0.8911 (14)	0.3412 (11)	−0.0987 (18)	6 (1)
O(64)	0.9277 (13)	0.1945 (09)	0.2771 (17)	5 (1)
C(1)	0.3193 (19)	0.2852 (13)	−0.053 (02)	4.1 (5)
C(2)	0.3605 (19)	0.2912 (13)	0.094 (02)	4.2 (5)
C(3)	0.296 (02)	0.2625 (15)	0.195 (03)	5.5 (6)
C(4)	0.362 (02)	0.3796 (16)	0.120 (03)	5.9 (7)
C(5)	0.460 (02)	0.2470 (17)	0.111 (03)	6.5 (7)
C(6)	0.6837 (19)	0.2152 (13)	0.399 (02)	4.0 (5)
C(7)	0.6422 (20)	0.2099 (14)	0.538 (02)	4.4 (5)
C(8)	0.713 (02)	0.2348 (14)	0.651 (03)	4.7 (6)
C(9)	0.543 (02)	0.2565 (15)	0.548 (03)	5.6 (6)
C(10)	0.639 (02)	0.1176 (16)	0.562 (03)	5.9 (7)
C(11)	0.355 (02)	0.0303 (15)	0.070 (03)	4.4 (6)
C(12)	0.1745 (19)	0.0414 (14)	0.161 (03)	4.0 (5)
C(13)	0.124 (02)	0.1860 (15)	0.042 (03)	4.5 (6)
C(14)	0.2929 (19)	0.1662 (13)	0.209 (03)	3.9 (5)
C(21)	0.1332 (18)	−0.0044 (13)	−0.384 (02)	3.4 (5)
C(22)	0.294 (02)	−0.0147 (15)	−0.204 (03)	4.5 (6)
C(23)	0.039 (02)	0.1173 (14)	−0.215 (02)	3.7 (5)
C(24)	0.1169 (17)	−0.0339 (13)	−0.101 (02)	3.2 (5)
C(31)	0.2889 (19)	0.2768 (14)	−0.403 (02)	3.8 (5)
C(32)	0.159 (02)	0.1648 (14)	−0.492 (03)	4.3 (6)
C(33)	0.3470 (19)	0.1040 (13)	−0.389 (02)	3.2 (5)
C(34)	0.132 (02)	0.2537 (14)	−0.255 (02)	3.9 (5)
C(41)	0.844 (02)	0.4537 (15)	0.632 (03)	4.8 (6)
C(42)	0.662 (02)	0.4743 (15)	0.524 (03)	4.5 (6)
C(43)	0.887 (02)	0.3081 (14)	0.518 (02)	3.5 (5)
C(44)	0.7227 (20)	0.3251 (14)	0.661 (03)	4.3 (5)
C(51)	0.962 (02)	0.3858 (13)	0.281 (02)	3.5 (5)
C(52)	0.708 (02)	0.5112 (15)	0.251 (03)	4.5 (6)
C(53)	0.8706 (20)	0.5060 (14)	0.094 (03)	4.4 (5)
C(54)	0.8870 (19)	0.5331 (14)	0.379 (03)	4.1 (5)
C(61)	0.7174 (19)	0.2244 (14)	0.054 (02)	3.9 (5)
C(62)	0.6567 (19)	0.3924 (13)	0.051 (02)	3.1 (5)
C(63)	0.8467 (18)	0.3310 (12)	−0.012 (02)	3.3 (5)
C(64)	0.8720 (19)	0.2427 (14)	0.227 (02)	3.7 (5)

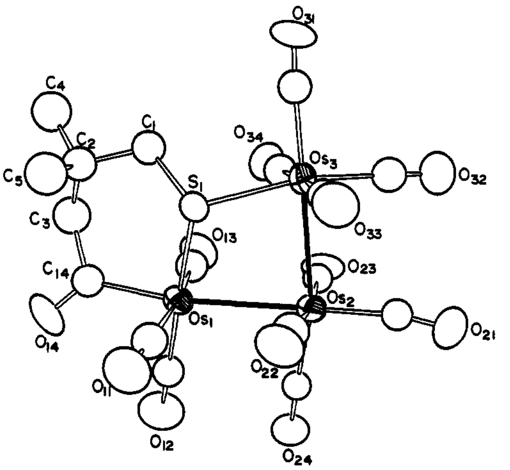

Figure 4. ORTEP diagram of $Os_3(CO)_{11}[\mu\text{-}SCH_2CMe_2CH_2C{=}O]$ (8), showing 50% probability thermal ellipsoids.

Table XII. Intramolecular Distances for 8[a]

Os(1)–Os(2)	3.005 (2)	Os(4)–C(44)	2.08 (3)
Os(1)–Os(3)	3.949 (2)	Os(5)–Os(6)	2.939 (2)
Os(1)–S(1)	2.431 (6)	Os(5)–C(51)	1.94 (3)
Os(1)–C(11)	1.97 (3)	Os(5)–C(52)	1.97 (3)
Os(1)–C(12)	1.91 (3)	Os(5)–C(53)	1.93 (3)
Os(1)–C(13)	1.91 (3)	Os(5)–C(54)	1.91 (3)
Os(1)–C(14)	2.10 (2)	Os(6)–S(2)	2.442 (6)
Os(2)–Os(3)	2.939 (2)	Os(6)–C(61)	1.91 (3)
Os(2)–C(21)	1.88 (2)	Os(6)–C(62)	2.01 (3)
Os(2)–C(22)	1.97 (3)	Os(6)–C(63)	1.93 (3)
Os(2)–C(23)	1.99 (3)	Os(6)–C(64)	1.97 (3)
Os(2)–C(24)	1.91 (2)	S(1)–C(1)	1.86 (2)
Os(3)–S(1)	2.448 (6)	S(2)–C(6)	1.85 (2)
Os(3)–C(31)	1.99 (3)	O(14)–C(14)	1.19 (3)
Os(3)–C(32)	1.95 (3)	O(44)–C(44)	1.27 (3)
Os(3)–C(33)	2.00 (3)	O–C(av)	1.13 (3)
Os(3)–C(34)	1.95 (3)	C(1)–C(2)	1.56 (3)
Os(4)–Os(5)	2.997 (2)	C(2)–C(3)	1.52 (4)
Os(4)–Os(6)	3.944 (2)	C(3)–C(14)	1.62 (3)
Os(4)–S(2)	2.436 (6)	C(6)–C(7)	1.55 (3)
Os(4)–C(41)	1.93 (3)	C(7)–C(8)	1.56 (3)
Os(4)–C(42)	1.97 (3)	C(8)–C(44)	1.53 (3)
Os(4)–C(43)	1.95 (3)		

[a] Distances are in angstroms. Estimated standard deviations in the least significant figure are given in parentheses.

Table XIII. Intramolecular Bond Angles for 8[a]

Os(2)–Os(1)–S(1)	80.5 (1)	S(1)–C(1)–C(2)	112 (2)
Os(2)–Os(1)–C(14)	171.2 (6)	C(1)–C(2)–C(3)	112 (2)
Os(1)–Os(2)–Os(3)	83.25 (5)	C(2)–C(3)–C(14)	118 (2)
Os(2)–Os(3)–S(1)	81.6 (1)	S(2)–C(6)–C(7)	113 (2)
Os(5)–Os(4)–S(2)	80.0 (1)	C(6)–C(7)–C(8)	111 (2)
Os(5)–Os(4)–C(44)	169.0 (7)	C(7)–C(8)–C(44)	117 (2)
Os(4)–Os(5)–Os(6)	83.26 (5)	Os(1)–C(14)–O(14)	126 (2)
Os(5)–Os(6)–S(2)	81.1 (1)	Os(1)–C(14)–C(3)	118 (2)
Os(1)–S(1)–Os(3)	108.1 (2)	O(14)–C(14)–C(3)	116 (2)
Os(1)–S(1)–C(1)	108.8 (8)	Os(4)–C(44)–O(44)	121 (2)
Os(3)–S(1)–C(1)	106.8 (8)	Os(4)–C(44)–C(8)	123 (2)
Os(4)–S(2)–Os(6)	107.9 (2)	O(44)–C(44)–C(8)	115 (2)
Os(4)–S(2)–C(6)	108.2 (8)	O–C(av)–Os	175 (2)
Os(6)–S(2)–C(6)	107.1 (8)		

[a] Angles are in degrees. Estimated standard deviations in the least significant figure are given in parentheses.

Tables IX and X. The complex contains an open cluster of three metal atoms. The nonbonding Os(1)⋯Os(3) distance is 3.937 (2) Å. There is a dimethylthiametallacyclopentane ring system with the sulfur atom S(1) bridging the open edge of the cluster. The metal–carbon distance to the methylene group C(3) is 2.16 (3) Å. The complex contains 11 linear terminal carbonyl ligands. The related complex $Os_3(CO)_{11}[\mu\text{-}SC(H)PhCH_2C(H)Ph]$ has been structurally characterized.[2] Complex 7 was converted back to 6 in 93% yield by irradiation-induced decarbonylation.

An ORTEP drawing of the molecular structure of 8 is shown in Figure 4. Final atomic positional parameters are listed in Table XI. Selected interatomic distances and angles are listed in Tables XII and XIII. The molecule consists of an open triosmium cluster with the sulfur atom

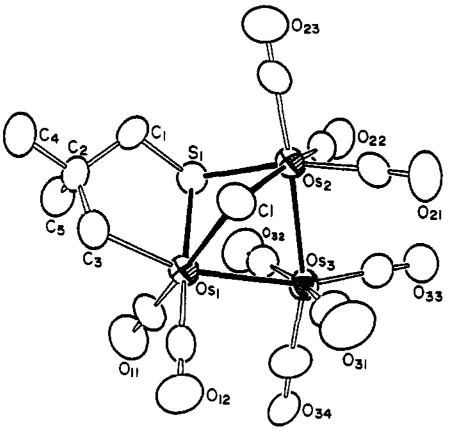

Figure 5. ORTEP diagram of the cluster anion $Os_3(CO)_9(\mu\text{-}Cl)[\mu\text{-}SCH_2CMe_2CH_2]^-$ (9), showing 50% probability thermal ellipsoids.

Table XIV. Positional Parameters and *B*(eq) Values (Å²) for 9

atom	*x*	*y*	*z*	*B*(eq)
Os(1)	0.62355 (04)	0.02170 (02)	0.74334 (02)	3.15 (2)
Os(2)	0.27539 (04)	0.01111 (02)	0.69118 (02)	3.38 (2)
Os(3)	0.41083 (04)	0.13371 (02)	0.76911 (02)	3.53 (2)
Cl	0.4347 (03)	−0.06999 (14)	0.77300 (14)	4.0 (1)
S(1)	0.4872 (03)	0.01842 (14)	0.62187 (13)	3.6 (1)
O(11)	0.8489 (09)	0.1263 (05)	0.7053 (05)	6.6 (5)
O(12)	0.7655 (09)	0.0097 (04)	0.9013 (04)	6.0 (4)
O(21)	0.0602 (08)	0.0180 (05)	0.8082 (05)	6.0 (4)
O(22)	0.1142 (08)	0.1231 (04)	0.5949 (04)	5.7 (4)
O(23)	0.1525 (09)	−0.1184 (05)	0.6007 (05)	7.4 (5)
O(31)	0.3901 (10)	0.0436 (05)	0.9121 (04)	7.0 (5)
O(32)	0.4884 (10)	0.1968 (05)	0.6179 (05)	7.1 (5)
O(33)	0.1320 (09)	0.2182 (05)	0.7738 (05)	6.5 (5)
O(34)	0.6275 (10)	0.2368 (05)	0.8488 (05)	7.9 (6)
N	0.9151 (09)	0.1759 (04)	0.0634 (04)	4.3 (4)
C(1)	0.5399 (11)	−0.0713 (05)	0.5915 (05)	3.8 (5)
C(2)	0.7028 (10)	−0.0802 (05)	0.6121 (05)	3.7 (5)
C(3)	0.7316 (10)	−0.0703 (06)	0.6983 (05)	4.0 (5)
C(4)	0.7455 (12)	−0.1560 (06)	0.5901 (06)	5.3 (6)
C(5)	0.7851 (12)	−0.0253 (06)	0.5705 (06)	5.3 (6)
C(11)	0.7607 (11)	0.0858 (06)	0.7197 (06)	4.2 (5)
C(12)	0.7113 (10)	0.0149 (05)	0.8399 (06)	3.9 (5)
C(21)	0.1371 (11)	0.0160 (06)	0.7631 (06)	4.3 (5)
C(22)	0.1749 (11)	0.0798 (06)	0.6331 (06)	4.1 (5)
C(23)	0.1999 (11)	−0.0708 (06)	0.6346 (06)	4.3 (5)
C(31)	0.3982 (12)	0.0762 (06)	0.8593 (06)	4.7 (6)
C(32)	0.4612 (12)	0.1709 (06)	0.6733 (07)	4.7 (6)
C(33)	0.2383 (13)	0.1855 (07)	0.7713 (06)	4.9 (6)
C(34)	0.5457 (14)	0.1962 (06)	0.8175 (06)	5.0 (6)
C(41)	1.0544 (14)	0.1344 (07)	0.0812 (07)	6.1 (7)
C(42)	1.1870 (14)	0.1825 (08)	0.0943 (08)	7.6 (8)
C(43)	0.9224 (14)	0.2229 (06)	−0.0044 (06)	5.7 (6)
C(44)	0.9608 (16)	0.1825 (08)	−0.0745 (07)	7.8 (8)
C(45)	0.7981 (13)	0.1191 (06)	0.0516 (06)	5.4 (6)
C(46)	0.6459 (14)	0.1477 (07)	0.0371 (07)	6.7 (7)
C(47)	0.8872 (13)	0.2265 (06)	0.1265 (06)	5.3 (6)
C(48)	0.8688 (13)	0.1890 (07)	0.2004 (06)	5.9 (6)

S(1) bridging the open edge, Os(1)⋯Os(3) = 3.949 (2) Å. It contains a thiametallacyclohexanone ring system that was formed by the insertion of CO into the metal–carbon bond of the metallacycle in 7. The osmium–carbon bond to the ketonic grouping is slightly shorter than the osmium carbon(methylene) bond in 7, Os(1)–C(14) = 2.10 (2) Å and C(14)–O(14) = 1.19 (3) Å. The complex contains 11 linear terminal carbonyl ligands. It can be converted back to 7 in good yields either by UV irradiation or by heating to 80 °C.

Table XV. Intramolecular Distances for 9[a]

Os(1)–Os(3)	2.9311 (8)	S(1)–C(1)	1.83 (1)
Os(1)–Cl	2.533 (3)	O–C(av)	1.16 (1)
Os(1)–S(1)	2.426 (2)	N–C(41)	1.52 (1)
Os(1)–C(3)	2.17 (1)	N–C(43)	1.50 (1)
Os(1)–C(11)	1.82 (1)	N–C(45)	1.52 (1)
Os(1)–C(12)	1.85 (1)	N–C(47)	1.51 (1)
Os(2)–Os(3)	2.8938 (8)	C(1)–C(2)	1.54 (1)
Os(2)–Cl	2.495 (3)	C(2)–C(3)	1.56 (1)
Os(2)–S(1)	2.427 (3)	C(2)–C(4)	1.52 (1)
Os(2)–C(21)	1.90 (1)	C(2)–C(5)	1.51 (1)
Os(2)–C(22)	1.85 (1)	C(41)–C(42)	1.52 (2)
Os(2)–C(23)	1.92 (1)	C(43)–C(44)	1.53 (2)
Os(3)–C(31)	1.95 (1)	C(45)–C(46)	1.52 (2)
Os(3)–C(32)	1.95 (1)	C(47)–C(48)	1.52 (1)
Os(3)–C(33)	1.87 (1)	Os(1)–Os(2)	3.303 (1)
Os(3)–C(34)	1.86 (1)		

[a] Distances are in angstroms. Estimated standard deviations in the least significant figure are given in parentheses.

Table XVI. Intramolecular Bond Angles for 9[a]

Os(3)–Os(1)–Cl	86.99 (6)	S(1)–Os(2)–C(23)	92.8 (3)
Os(3)–Os(1)–S(1)	81.44 (6)	Os(1)–Os(3)–Os(2)	69.08 (2)
Os(3)–Os(1)–C(3)	162.8 (3)	Os(1)–Os(3)–C(31)	80.6 (3)
Os(3)–Os(1)–C(11)	94.3 (3)	Os(1)–Os(3)–C(32)	83.7 (3)
Os(3)–Os(1)–C(12)	98.6 (3)	Os(1)–Os(3)–C(33)	163.2 (3)
Cl–Os(1)–S(1)	81.56 (8)	Os(1)–Os(3)–C(34)	94.2 (4)
Cl–Os(1)–C(3)	84.7 (3)	Os(2)–Os(3)–C(31)	85.3 (3)
Cl–Os(1)–C(11)	178.2 (3)	Os(2)–Os(3)–C(32)	88.8 (3)
Cl–Os(1)–C(12)	90.9 (3)	Os(2)–Os(3)–C(33)	94.1 (3)
S(1)–Os(1)–C(3)	82.5 (3)	Os(2)–Os(3)–C(34)	163.3 (4)
S(1)–Os(1)–C(11)	97.5 (3)	Os(1)–Cl–Os(2)	82.12 (8)
S(1)–Os(1)–C(12)	172.5 (3)	Os(1)–S(1)–Os(2)	85.79 (8)
C(3)–Os(1)–C(11)	93.7 (4)	Os(1)–S(1)–C(1)	99.0 (3)
C(3)–Os(1)–C(12)	96.6 (4)	Os(2)–S(1)–C(1)	110.7 (3)
Os(3)–Os(2)–Cl	88.53 (6)	C–N–C(av)	109.5 (9)
Os(3)–Os(2)–S(1)	82.19 (6)	S(1)–C(1)–C(2)	108.1 (7)
Os(3)–Os(2)–C(21)	85.9 (3)	C(1)–C(2)–C(3)	107.8 (7)
Os(3)–Os(2)–C(22)	85.0 (3)	C(1)–C(2)–C(4)	108.2 (8)
Os(3)–Os(2)–C(23)	175.0 (3)	C(1)–C(2)–C(5)	110.1 (8)
Cl–Os(2)–S(1)	82.31 (8)	C(2)–C(2)–C(4)	109.9 (8)
Cl–Os(2)–C(21)	91.9 (3)	C(3)–C(2)–C(5)	111.2 (8)
Cl–Os(2)–C(22)	172.9 (3)	C(4)–C(2)–C(5)	109.6 (8)
Cl–Os(2)–C(23)	90.5 (3)	Os(1)–C(3)–C(2)	114.7 (6)
S(1)–Os(2)–C(21)	166.8 (3)	Os–C–O(av)	179 (1)
S(1)–Os(2)–C(22)	93.9 (3)	N–C–C(av)	114 (1)

[a] Angles are in degrees. Estimated standard deviations in the least significant figure are given in parentheses.

Complex 6 also reacts with Cl^- at 25 °C to produce the chloride-bridged salt $[Os_3(CO)_9(\mu\text{-}SCH_2C(Me)_2CH_2)(\mu\text{-}Cl)]^-[(Et)_4N]^+$ (9) in 87% yield. Compound 9 was characterized crystallographically, and an ORTEP drawing of the molecular structure of the cluster anion 9 is shown in Figure 5. Final atomic positional parameters are listed in Table XIV. Selected interatomic distances and angles are listed in Tables XV and XVI. The molecule consists of an open triosmium cluster with a chloro ligand bridging the open edge, Os(1)–Cl = 2.533 (3) Å and Os(2)–Cl = 2.495 (3) Å. There is a dimethylthiametallacyclopentane ring system similar to that in 7 with the sulfur atom also bridging the open edge, Os(1)–C(3) = 2.17 (1) Å. Since there are two ligands bridging the nonbonding Os(1)⋯Os(2) interaction, the distance is shortened considerably to 3.303 (1) Å compared to that in 7. The chloride addition was accompanied by a decarbonylation; thus, the complex contains only nine carbonyl ligands.

Discussion

The cluster-assisted ring opening of thietanes containing hydrogen atoms in the 3-position is followed by CH activation that occurs through a β-elimination mechanism in a metallacyclic intermediate.[1] With 3,3-dimethylthietane this CH activation step is prohibited. Ring opening by cleavage of a carbon–sulfur bond is the first step in the photochemical transformation of the 3,3-DMT ligand in 2. This yields the thiametallacyclic complex 6.

Scheme I

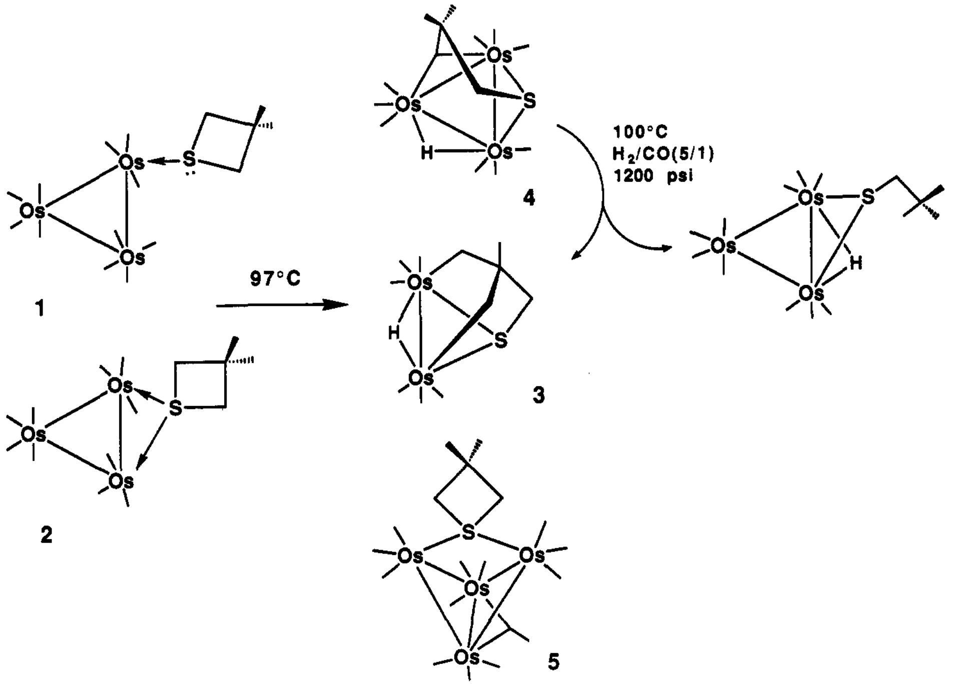

Scheme II

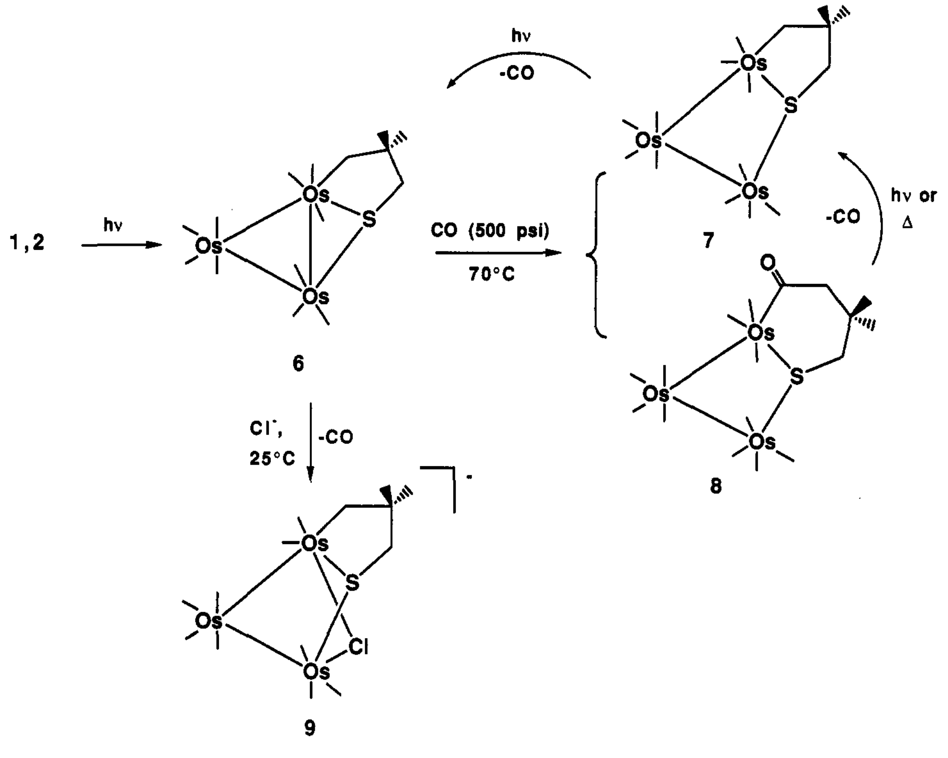

Presumably, this is also the first step in the thermally induced ring-opening transformation, but at the temperature required to initiate that reaction (97 °C), a further transformation involving loss of a CO ligand and an α-CH activation occurs to yield the complex 4, as shown in Scheme I. In an independent experiment it was shown that 6 is readily transformed to 4 at 97 °C. It is noteworthy that in the irradiation of 1 a significant amount of complex 2 was also isolated. This suggests that decarbonylation of 1 to 2 is probably the first step in the transformations of 1.

The thermal transformation of 2 also yields the dinuclear complex 3 and tetranuclear complex 5 by a fragmentation and an aggregation reaction. The formation of 3 involves a γ-CH activation on one of the methyl groups. Compound 3 can also be obtained from 4 at 100 °C under a mixture of CO/H_2 (1/5 at 1200 psi) and must involve a reversal of the α-CH activation process that led to 4. The reversal of the α-CH activation is also implicit in the formation of the neopentanethiolate-containing product $Os_3(CO)_{10}[\mu\text{-}SCH_2CMe_3](\mu\text{-}H)$ obtained in the same reaction.

Under the pressure of CO alone 6 is carbonylated in two steps; see Scheme II. The first step is simply a CO-induced cleavage of the sulfur-bridged metal–metal bond to yield 7. A similar cluster opening occurred for the addition of CO to $Os_3(CO)_{10}[\mu\text{-}SC(H)PhCH_2C(H)Ph]$ (B).[2] The second step is a CO insertion reaction into the metal–carbon bond of the thiametallacycle to yield complex **8** containing an acyl function. Both of these steps can be reversed by mild heating or by the application of UV–vis irradiation. We have observed a similar CO insertion into the complex $Os_3(CO)_{10}[(\mu\text{-}SCH_2CMe_2CH_2)_3]$.[4] However, in that example the keto function bridges the cluster in a μ-η^2 mode.

Alper et al. have produced γ-thiobutyrolactones catalytically via regiospecific carbonylations of thietane, 2-methylthietane, and 3-methoxythietane using cobalt and ruthenium carbonyls as catalyst precursors.[16] We believe that compounds **6** and **8** provide viable models for intermediates that might be involved in the catalytic reactions observed by Alper. Efforts to obtain further support for this are in progress.

In related studies we have shown that nucleophiles including Cl^- add directly to the bridging 3,3-DMT ligand in complex **2** to open the thietane ring through cleavage of a carbon–sulfur bond.[4,5] Herein, we have demonstrated that the addition of Cl^- to the thiametallacyclic complex **6** proceeds by addition to the metal atoms and not to the opened thietane ligand. Thus, the thiametallacycle in **6** is not as susceptible to nucleophilic addition as is the intact, bridging 3,3-DMT ligand in **2**.

Acknowledgment is made to the donors of the Petroleum Research Fund, administered by the American Chemical Society, and the Office of Basic Energy Sciences of the U.S. Department of Energy for support of this research.

Supplementary Material Available: Tables of hydrogen atom positional parameters and anisotropic thermal parameters (15 pages). Ordering information is given on any current masthead page. Structure factor tables for the structural analyses of compounds **3**, **4**, and **9** were deposited previously.[3,4a]

OM9211733

---

[16] Wang, M. D.; Calet, S.; Alper, H. *J. Org. Chem.* **1989**, *54*, 20.

Reactions of Amides with Zerovalent and Divalent Palladium and Platinum Complexes

David R. Schaad and Clark R. Landis*

Departments of Chemistry and Biochemistry, University of Colorado—Boulder, Boulder, Colorado 80309, and Department of Chemistry, University of Wisconsin, Madison, Wisconsin 53706

Received October 21, 1991

The reactions of amides ($RCONH_2$ and $CF_3SO_2NH_2$) with $L_2Pd(CH_3)_2$ and $L_2Pt(CH_3)_2$ and with transient L_2Pt^0 to yield new complexes containing palladium– and platinum–amido nitrogen bonds are reported. Photolysis of $Pt(C_2O_4)(PEt_3)_2$ (**1**) in the presence of amide generates products of the type *trans*-$PtH(HNR)(PEt_3)_2$ (R = SO_2CF_3 (**1a**), $COCF_3$ (**1b**)). Reaction of amides with *trans*-$PtH(CH_3)(PEt_3)_2$ (**2**), *cis*-$PdMe_2(PEt_3)_2$ (**3**), *cis*-$PtMe_2(PEt_3)_2$ (**4**), $PdMe_2(dcpe)$ (**5**), $PdMe_2(dmpe)$ (**6**), and $PtMe_2(COD)$ (**7**) produces **1a**,**b**, *trans*-$PdMe(HNR)(PEt_3)_2$ (R = SO_2CF_3 (**3a**), $COCF_3$ (**3b**), $COCF_2H$ (**3c**), COPh (**3d**)), $PtMe(HNR)(PEt_3)_2$ (R = SO_2CF_3 (**4a**), $COCF_3$ (**4b**)), PdMe(HNR)(dcpe) (R = SO_2CF_3 (**5a**), $COCF_3$ (**5b**), COPh (**5c**)), $PdMe(HNSO_2CF_3)(dmpe)$ (**6a**), and PtMe(HNR)(COD) (R = SO_2CF_3 (**7a**), $COCF_3$ (**7b**)), respectively. The stereochemistry and topologies of the new compounds are established by multinuclear NMR spectroscopy. The relevance of these reactions to hydroamination catalysis is discussed.

Introduction

The activation of N–H bonds[1] by transition-metal complexes[2] is an integral feature of recent developments in hydroamination catalysis.[3,4] Our research on the design of new hydroamination catalysts has focused on the reactions of amides at metal centers because (1) amides are synthetic equivalents of the simplest hydroamination reagent, ammonia, and (2) the relatively high acidity of amide vs ammonia N–H bonds may provide a lower energy pathway for metal-facilitated functionalization. We have previously reported that amides react with *cis*-$FeH_2(dmpe)_2$, $FeH(C_6H_4PPhCH_2CH_2PPh_2)(dppe)$, and *cis*-$RuH(naphthyl)(dmpe)_2$ (dmpe = 1,2-bis(dimethylphosphino)ethane; dppe = 1,2-bis(diphenylphosphino)ethane) to generate *trans*-$M(H)(RNH)(diphosphine)_2$ complexes.[5] Herein we report the extension of these studies to zerovalent and divalent palladium and platinum compounds containing phosphine and olefin ligands.

Steps relevant to hydroamination catalysis include transition-metal-promoted N–H bond activation, insertion of an olefin into a M–C or M–N bond, and reductive elimination or protonolysis to form the hydroamination product and regenerate the catalyst. We report the re-

---

* To whom correspondence should be addressed at the University of Wisconsin.

[1] Herein we use the term N–H bond activation to indicate cleavage of an N–H bond induced by a metal center via homolytic cleavage, heterolytic cleavage, or oxidative addition.

[2] (a) Roundhill, D. M *Inorg. Chem.* **1970**, *9*, 254. (b) Nelson, J. H.; Schmidt, J. L.; Henry, R. A.; Moore, D. W.; Jonassen, H. B. *Inorg. Chem.* **1970**, *9*, 2678. (c) Sappa, E.; Milone, L. *J. Organomet. Chem.* **1973**, *61*, 383. (d) Rauchfuss, T. B.; Roundhill, D. M. *J. Am. Chem. Soc.* **1974**, *96*, 3098. (e) Bryan, E. G.; Johnson, B. F. G.; Lewis, J. *J. Chem. Soc., Dalton Trans.* **1977**, 1328. (f) Fornies, J.; Green, M.; Spencer, J. L.; Stone, F. G. A. *J. Chem. Soc., Dalton Trans.* **1977**, 1006. (g) Susa-Fink, G. *Z. Naturforsh., B: Anorg. Chem., Org. Chem.* **1980**, *35B*, 454. (h) Johnson, B. F. G.; Lewis, J.; Odiaka, T. I.; Raithby, P. R. *J. Organomet. Chem.* **1981**, *216*, C56. (i) Yamamoto, T.; Sano, K.; Yamamoto, A. *Chem. Lett* **1982**, 207. (j) Hedden, D.; Roundhill, D. M.; Fultz, W. C.; Rheingold, A. L. *J. Am. Chem. Soc.* **1984**, *106*, 5014. (k) Hillhouse, G. L.; Bercaw, J. E. *J. Am. Chem. Soc.* **1984**, *106*, 5472. (l) Lin, Y. C.; Mayr, A.; Knobler, C. B.; Kaesz, H. D. *J. Organomet. Chem.* **1984**, *272*, 207. (m) Park, S.; Hedden, D.; Roundhill, D. M. *Organometallics* **1986**, *5*, 2151. (n) Bercaw, J. E.; Davies, D. L.; Wolczanski, P. T. *Organometallics* **1986**, *5*, 443. (o) Casalnuovo, A. L.; Calabrese, J. C.; Milstein, D. *Inorg. Chem.* **1987**, *26*, 971. (p) Walsh, P. J.; Hollander, F. J.; Bergman, R. G. *J. Am. Chem. Soc.* **1988**, *110*, 8729. (q) Park, S.; Johnson, M. P.; Roundhill, D. M. *Organometallics* **1989**, *8*, 1700. (r) Ladipo, F. T.; Merola, J. S. *Inorg. Chem.* **1990**, *29*, 4172. (s) Hursthouse, M. B.; Mazid, M. A.; Robinson, S. D.; Sahajpal, A. *J. Chem. Soc., Chem. Commun.* **1991**, 1146.

[3] Casalnuovo, A. L.; Calabrese, J. C.; Milstein, D. L. *J. Am. Chem. Soc.* **1988**, *110*, 6738.

0276-7333/92/2311-2024$03.00/0